JCTC Journal of Chemical Theory and Computation

pubs.acs.org/JCTC Article

Accelerating Anharmonic Spectroscopy Simulations via Local-Mode, Multilevel Methods

Asylbek A. Zhanserkeev, Emily L. Yang, and Ryan P. Steele*

Cite This: *J. Chem. Theory Comput.* 2023, 19, 5572−5585 Read Online

ACCESS | Metrics & More | Article Recommendations | Supporting Information

ABSTRACT: *Ab initio* computer simulations of anharmonic vibrational spectra provide nuanced insight into the vibrational behavior of molecules and complexes. The computational bottleneck in such simulations, particularly for *ab initio* potentials, is often the generation of mode-coupling potentials. Focusing specifically on two-mode couplings in this analysis, the combination of a local-mode representation and multilevel methods is demonstrated to be particularly symbiotic. In this approach, a low-level quantum chemistry method is employed to predict the pairwise couplings that should be included at the target level of theory in vibrational self-consistent field (and similar) calculations. Pairs that are excluded by this approach are "recycled" at the low level of theory. Furthermore, because this low-level pre-screening will eventually become the computational bottleneck for sufficiently large chemical systems, distance-based truncation is applied to these low-level predictions without substantive loss of accuracy. This combination is demonstrated to yield sub-wavenumber fidelity with reference vibrational transitions when including only a small fraction of target-level couplings; the overhead of predicting these couplings, particularly when employing distance-based, local-mode cutoffs, is a trivial added cost. This combined approach is assessed on a series of test cases, including ethylene, hexatriene, and the alanine dipeptide. Vibrational self-consistent field (VSCF) spectra were obtained with an RI-MP2/cc-pVTZ potential for the dipeptide, at approximately a 5-fold reduction in computational cost. Considerable optimism for increased accelerations for larger systems and higher-order couplings is also justified, based on this investigation.

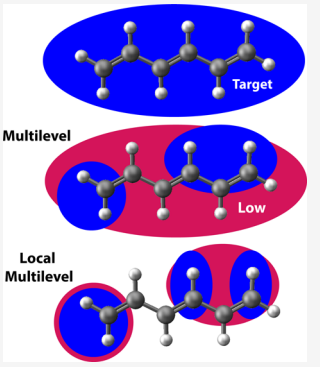

INTRODUCTION

Infrared and Raman spectroscopies provide detailed glimpses into the behavior of molecules and, implicitly, the potential energy and dipole surfaces that govern their vibrational dynamics. Recent progress in cold-ion sources and action spectroscopies has generated unprecedented insight into ion hydration, hydrogen bonding, and biomolecular structure.[1−13] Advanced theory and computational simulations have become critical partners in the interpretation of these modern experiments,[1,4,5,7,14−22] and the present investigation aims to address the suitability of a combination of new computational approaches for molecules and clusters of the size accessed by these experiments. In this somewhat expanded Introduction section, the details of these methods will be reviewed, along with the reasons that this pairing of methods is particularly symbiotic for anharmonic simulations of large systems.

A suite of methods now exists for this purpose, ranging from variational solvers[17−20,23] on all or a targeted subset of vibrational modes to more general methods that are often analogues of well-known methods in electronic structure theory. Mean-field methods, such as the vibrational self-consistent field[21,24−35] (VSCF) method, can be supplemented by mode-correlation corrections, including perturbation theories (VMP2[36,37] and VDPT2[38]), configuration interaction[21,25,32,33,39−41] (VCI), and coupled-cluster theories[32,42−44] (VCC); direct correlations from a harmonic reference are also possible.[45−47] The success of these methods on reasonably small chemical systems—provided that spectroscopically accurate potential energy surfaces are employed (typically involving large basis sets and correlated-electron wavefunctions)—engenders considerable optimism for their ability to lend insight to the types of systems now accessed with the aforementioned experiments,[48−50] including large ion hydrates, biomolecules, and pharmaceuticals.[51−56]

The general applicability of these approaches is severely limited, however, by the practical need for nonlocal (or at least semilocal) representations of the governing potential surface. The ostensibly exponential scaling of such representations has limited these techniques to relatively small molecules/complexes[19,20] or small subspaces of larger molecules.[35] One of the standard routes to reducing this complexity is the "n-mode representation" (n-MR),[22,26,28] which is effectively a many-body expansion in the space of vibrational modes (in selected vibrational coordinates, $\{q\}$, for an N-atom system):

Received: June 1, 2023
Published: August 9, 2023

https://doi.org/10.1021/acs.jctc.3c00589
J. Chem. Theory Comput. 2023, 19, 5572−5585

$$V(q_1, q_2, \cdots, q_{3N-6}) = V_0 + \sum_{i}^{3N-6} V^{(1)}(q_i) + \sum_{i}^{3N-6} \sum_{j>i}^{3N-6} \Delta V^{(2)}(q_i, q_j) + \sum_{i}^{3N-6} \sum_{j>i}^{3N-6} \sum_{k>j}^{3N-6} \Delta V^{(3)}(q_i, q_j, q_k) + \cdots \quad (1)$$

The 1-body ("1-MR") terms are composed of one-dimensional cuts along vibrational modes, and although these cuts form intuitive low-dimensional images of anharmonicity, they are often qualitatively incorrect—at least in rectilinear displacements—and often even yield the wrong sign of the anharmonicity. Instead, higher-order couplings, such as the pairwise couplings ("2-MR") of all modes in $\Delta V^{(2)}$, provide the necessary anharmonic corrections that properly account for the strong anharmonicities and resonant effects that can qualitatively alter spectra from their harmonic reference. The need for these 2-MR (and higher) coupling terms presents the central computational challenge for anharmonic spectroscopy simulations, as the inclusion of these terms requires nonlocal quadrature, Taylor expansions, or statistical sampling. Precedent on small test systems has indicated that this *n*-MR expansion sufficiently converges by approximately the 4-body terms[22] (which is already an enormous success over full, *n*-dimensional representations), although computational cost considerations often limit this expansion to 2-MR.[35] This latter limitation is problematic for two reasons. First, 2-MR potentials can sometimes exhibit qualitative deficiencies in cases of strong coupling.[57] Second, and perhaps more relevant to the present analysis, is the fact that even 2-MR potentials can be many orders of magnitude more costly than their harmonic reference calculation and cost-prohibitive for molecules of even modest size when using spectroscopically accurate, *ab initio* potentials. As a tangible example to be examined in more detail later in this work, the alanine dipeptide—a small molecule by biochemical standards—would require 2.1×10^5, 4.6×10^7, and 7.1×10^9 potential energy evaluations for 2-, 3-, and 4-MR potentials, respectively, even when using efficient Gauss−Hermite quadrature schemes.[58] Progress in grid-reduction schemes has occurred[59−64]—and these improvements are directly amenable to the methods presented herein—but the overall scaling of the *n*-MR nonetheless remains prohibitive for large molecules.

Local-Mode Methods. The rapid growth in mode-coupling terms is a rather artificial pathology. In canonical, delocalized, normal-mode coordinates, no *a priori* means of predicting the strength of these couplings exists, and indeed, such growth is observed in practice. This notion conflicts with the basic chemical/physical concept, however, that localized vibrational motions should not appreciably couple to other localized vibrational motions at long distances. Such concepts form the basis of chemists' nomenclature for vibrational modes but are not borne out in the canonical normal modes that are often used to compute them, particularly for larger molecules where degeneracy induces the motion of nearly all atoms within a normal-mode representation.

An understanding of these issues formed the foundation for the development of generalized local-mode methods. Although originally employed to disentangle the harmonic spectra of large molecules,[65,66] automatically generated local modes address the scaling bottleneck by directly exploiting the rapid distance decay of the coupling between local vibrational motions.[67−74] Put simply, localized motions do not couple strongly (or, often, even weakly) to distant vibrations, and, therefore, only modes within a surprisingly short-distance cutoff are necessary for converged anharmonic simulations. In two proof-of-concept analyses from our group,[67,68] for example, sub-wavenumber fidelity with cutoff-free simulations could be obtained with 8 Bohr (4.2 Å) cutoffs and 2-MR potentials, yielding 2- to 5-fold speedups for modest-sized molecules and considerable potential for enhanced accelerations on larger molecules. Even shorter-range cutoffs and multiple-order-of-magnitude accelerations were demonstrated for 3-MR potentials. Recent analyses have also demonstrated considerable transferability of the couplings between local vibrational modes in C−H stretch models, for example.[50,75,76]

As a demonstrative example of this locality for the present investigation, the two-mode couplings for hexatriene, $H_2C(CH)_4CH_2$ are depicted in Figure 1. For this analysis, the root-mean-squared coupling definition, $\langle 00|\Delta V^{(2)}|00\rangle^{1/2}$ from ref 67 is employed (where the integration is performed over the harmonic ground-state wavefunctions for the sake of transferability), although many other alternatives exist.[59,77−81] The distance decay of these couplings is clearly evident in Figure 1, even for a molecule with relatively little "room" for such distance dependence. The distance-based cutoffs of refs 67 and 68—depicted by the horizontal arrow in Figure 1—remove the long-range, small-value couplings and accelerate a 2-MR by a modest 28% for this small molecule if using an 8 Bohr cutoff. For larger molecules, the number of mode pairs comprising the long-distance tail increases more rapidly than the density of short-range pairs. In this sense, a local-mode framework appears to be a promising approach for extending anharmonic simulation methods to large systems, and it also carries several other now-established, ancillary benefits for correlated-mode calculations.[33,69,70,79,82−86]

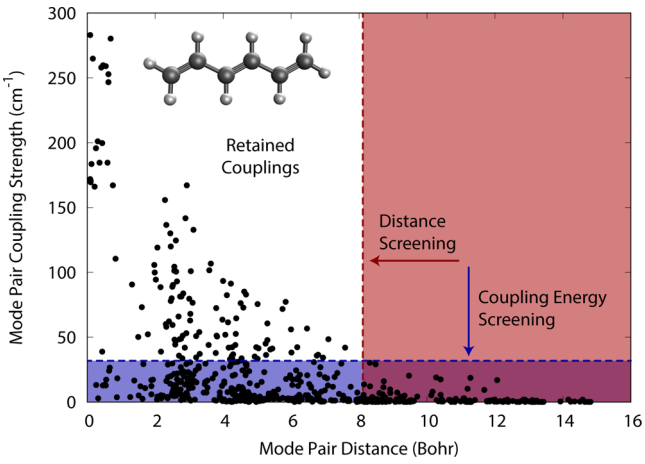

Figure 1. Integrated two-mode coupling values for a local-mode representation of vibrations in hexatriene, as a function of distance between mode centers. Also depicted schematically are the distance- and energy-based approaches to screening mode couplings.

This distance-based pruning has been demonstrated to be both transferrable and efficient, particularly for larger molecules, but it is not without limitations. In particular, extant inefficiencies exist in the small-value couplings that are observed at distances inside the cutoff. These couplings represent terms that happen to vanish by symmetry or other more physical origins, such as high-frequency modes adiabatically "following"

https://doi.org/10.1021/acs.jctc.3c00589
J. Chem. Theory Comput. 2023, 19, 5572−5585

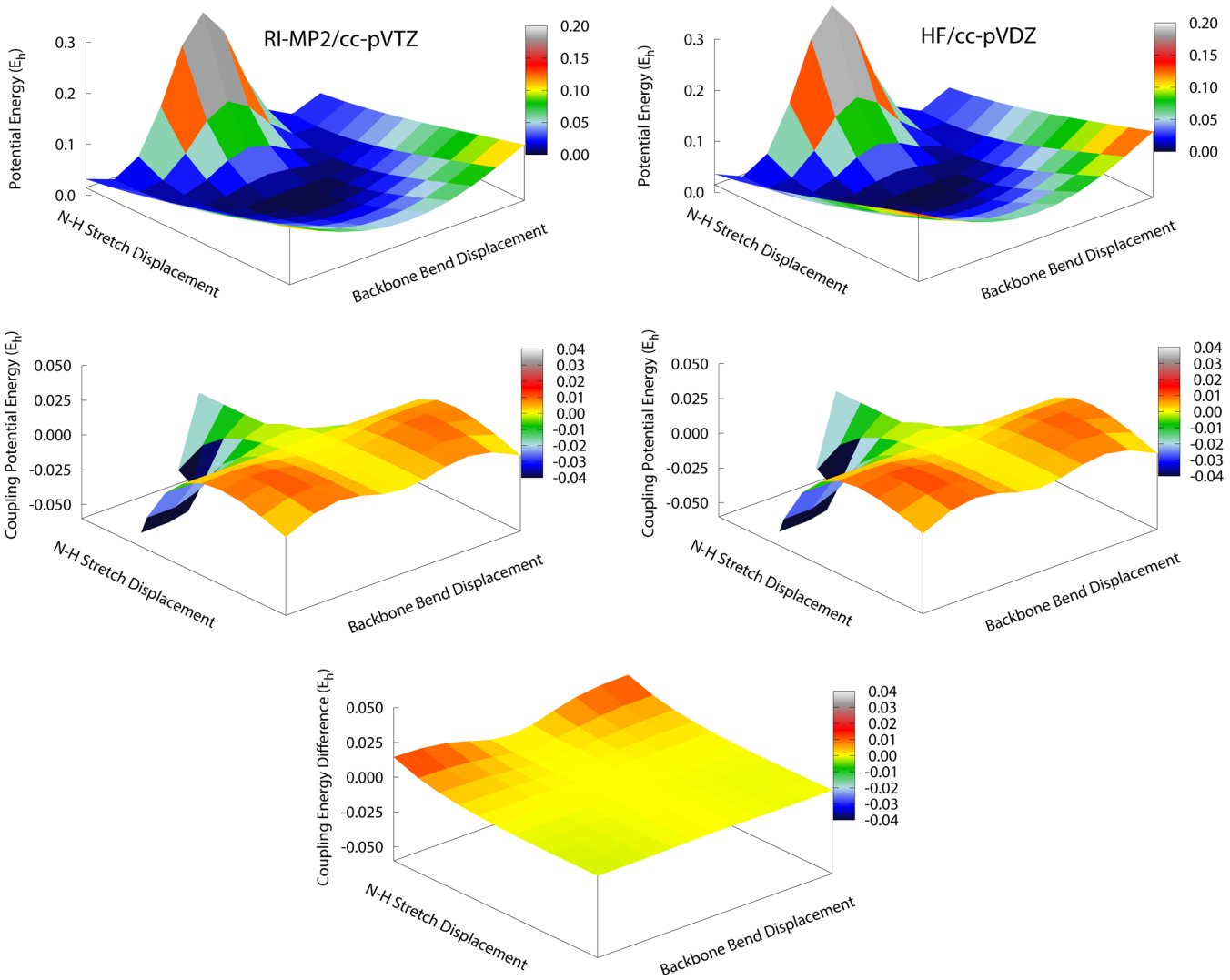

Figure 2. Two-mode potentials for the hydrogen-bonded N−H stretch and backbone bend vibrations in Ala_2 for the RI-MP2/cc-pVTZ (left) and HF/cc-pVDZ (right) methods. Top row: Total two-mode potentials. Middle row: Coupling potentials $\Delta V^{(2)}$. Bottom: Difference between low- and target-level coupling potentials. Data points are computed at the same Gauss−Hermite quadrature points as described in the Methods section.

nearby low-frequency motions. If some means existed to efficiently predict such scenarios, then an additional pre-screening—the vertical arrow in Figure 1—could be applied to the local-mode methods to isolate only the short-range and strong-coupling pairs that substantively impact anharmonic spectral simulations. This battle-on-two-fronts approach forms the foundation of the methodology presented in this work. After unsuccessfully pursuing physics-based approaches for predicting the existence of these short-range/low-coupling pairs (although we do not rule out the existence of such methods), we have instead opted for a more pragmatic alternative. Namely, we exploit the now-well-known observation that mode couplings feature little sensitivity to the underlying quantum chemistry method, even in cases when the low-order, single-mode scans exhibit such sensitivity.[32,34,59,62,77,79,87−96]

This marriage of local-mode and multilevel/screening methods will be shown to be a particularly appropriate combination of techniques and a pairing that is better than the sum of its parts, for reasons explained below. In some sense, this approach is philosophically consistent with recent approaches to analytic potential fitting,[97−102] wherein short-range, quantum effects are sufficiently complex to require fits with modern polynomial approaches,[103,104] whereas long-range effects are fit to more standard functional forms and many-body polarization terms.

Multilevel and Pre-Screening Methods. In multilevel approaches to anharmonic vibrational spectroscopy (also sometimes termed "multiresolution" or "hybrid" methods), at least some terms in the *n*-MR potential are represented—or pre-screened—by more cost-efficient potential energy surfaces. These methods received their first systematic analyses in the early 2000s,[59,62,77,78,89,90,92,94,96,105,106] although examples of their use in Taylor series potentials occurred at least a decade prior,[87,88] and development has continued since.[32,34,79,91,93,95,107,108] These approaches are considered in the context of local-mode methods in the present work as a particularly attractive means to distinguish the remnant short-range couplings that were discussed in the preceding section.

As a simple example in the *n*-MR context, a multilevel 2-MR might be employed as

$$V^{(2)} = \sum_i V^{(1)}_{\text{target}}(q_i) + \sum_i \sum_{j>i} \Delta V^{(2)}_{\text{low}}(q_i, q_j) \tag{2}$$

https://doi.org/10.1021/acs.jctc.3c00589
J. Chem. Theory Comput. 2023, 19, 5572−5585

where the 1- and 2-MR terms are represented by target-level and low-level potentials, respectively. Alternatively (or possibly in concert), some of the mode-coupling pairs could be represented by $\Delta V^{(2)}_{\text{target}}$ based on initial estimates from $\Delta V^{(2)}_{\text{low}}$. Both approaches will be investigated in the present work.

A variety of low-level methods have historically been employed for these purposes, including Hartree−Fock or density functional theory methods,[59,89,90,95] Harris functionals,[94] and even semiempirical methods.[78,109] Cancellation of the nuanced quantum chemistry detail of the differential coupling terms $\Delta V^{(2)}$ (much of which was already captured in the 1-MR cuts $V^{(1)}$) forms the underlying premise of these approaches. Indeed, we have found this premise to be surprisingly accurate for the test systems considered in this work (details in the Methods section). For example, both the two-dimensional total and coupling surfaces of a strongly coupled pair in the alanine dipeptide, Ala_2, involving the intramolecular hydrogen-bond stretch motion and a backbone bend motion, are depicted in Figure 2 (left) for the RI-MP2/cc-pVTZ quantum chemistry method. The coupling surface is decidedly not flat, which is indicative of the strong pairwise coupling behavior among these motions. The analogous surfaces with the more economical HF/cc-pVDZ method are depicted in Figure 2 (right). Despite the harmonic H-bond stretch fundamental shifting by 283 cm^{-1} between these two methods, the surfaces—including the coupling surfaces—are visually indistinguishable on the scale of these plots. In fact, the difference surface (subtracting the two coupling surfaces, $\Delta\Delta V^{(2)}$), shown in Figure 2(bottom), only exhibits substantive deviations (<0.015 E_h) at the corners of the quadrature grid, where the two-dimensional vibrational basis functions contribute little anyway.

The choice of the low-level method, of course, impacts both the quality and efficiency of the multilevel approach. Although the purpose of the present analysis is not to exhaustively test the necessary requirements for a low-level prior, the coupling data presented in Figure 3 provides a preliminary sense of this sensitivity. The integrated RMS couplings for all unique mode pairs of the same Ala_2 example are depicted for the reference RI-MP2/cc-pVTZ method and three low-level alternatives.

The main outcome of this brief examination is that the trend in coupling strengths is well represented by all low-level methods. Reduction in only the basis set (RI-MP2/cc-pVDZ) shows modest quantitative deviations for only the strongest couplings, and additional removal of electron correlation (HF/cc-pVDZ) exhibits very similar behavior. These two methods exhibit 14-fold and 60-fold accelerations of the potential energy surface computation, respectively. Even the particularly crude HF/STO-3G approach (2800 times faster than the reference RI-MP2/cc-pVTZ method) provides a near-linear correlation with target-level coupling values, albeit with a nonunity slope. (The near-linear behavior of all depicted methods is related to recent multilevel methods that empirically scale the low-level potential.[95])

For these reasons, a combination of low- and high-level methods is employed for two purposes in the present work. Based on the accurate prediction of strongly coupled mode pairs by low-level methods, they will be used in a pre-screening capacity to determine the mode pairs that are included at the target level of theory. Given that these estimates of the coupling border on quantitative, however, neglecting the small couplings altogether when they fall below an empirically determined cutoff appears wasteful. Therefore, in this work, we also examine the possibility of "recycling" these low-level coupling terms after pre-screening, as a sufficient estimate of the smaller couplings.

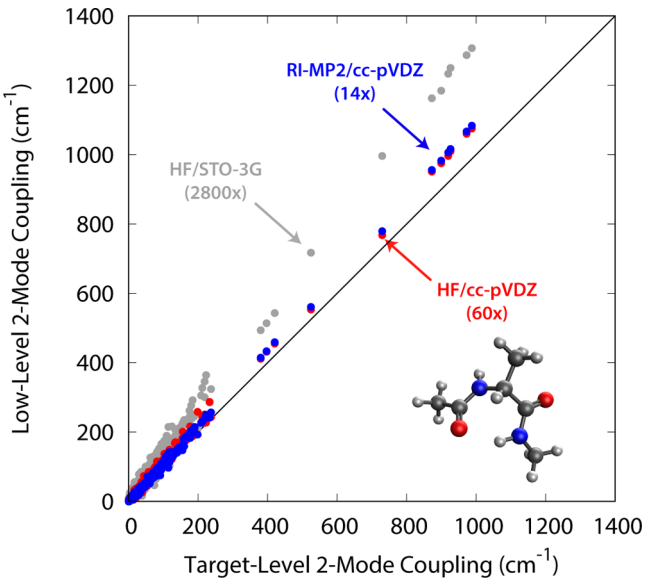

Figure 3. Comparison of integrated two-mode couplings from the RI-MP2/cc-pVTZ (target) method and three low-level alternatives for Ala_2. Each data point corresponds to a mode pair's couplings from low- and target-level methods. The diagonal line corresponds to equal couplings between methods. The parenthetical numerical values indicate the computational acceleration engendered by each low-level method, compared to the target-level method.

Motivation for Combination of Methods. Multilevel/pre-screening methods can be used to eliminate the short-range, small-value couplings that distance truncations alone can sometimes overlook, and therefore, a combination of the two methods seems particularly appropriate. Furthermore, as will be discussed later, computations on larger systems can actually yield scenarios in which the low-level pre-screening can become the computational bottleneck. The distance-based, local-mode truncation scheme alleviates this bottleneck and holds considerable promise for calculations on larger chemical systems.

One previous investigation[79] considered an approach akin to this combination. The distinctions in this alternative approach were that it was performed for small molecules (up to 8 atoms) without low-level recycling, with localization only of C−H stretching modes, and with the remaining modes retained as canonical normal modes. This analysis demonstrated little improvement due to locality, but this outcome was likely expected, given the size of the systems involved. Similarly, Klinting et al[108] systematically analyzed a combination of alternative coordinate schemes and pre-screening on maleimide (10 atoms), although the ability to pre-screen the low-level potential, based on mode distances, was not pursued.

The present investigation was intentionally designed to focus on the behavior of pairwise, 2-MR couplings in the context of this multilevel, local-mode methodology. This choice was made because (a) these couplings often make the largest contributions to anharmonicity, and (b) any accelerations demonstrated in this analysis would represent a considerable lower bound to savings observed at higher orders of the n-MR expansion. Prospects for the latter will be discussed in the Conclusions section.

https://doi.org/10.1021/acs.jctc.3c00589
J. Chem. Theory Comput. 2023, 19, 5572−5585

METHODS

The basic computational method examined here is a reasonably straightforward combination of the local-mode and multilevel/pre-screening methods described in the Introduction section:

(1) The pre-screening of two-mode couplings in a 2-MR is performed using a suitably chosen low-level potential, as a means of predicting the "important" couplings at a target level of theory. Using the RMS definition of the couplings, mode pairs are either neglected altogether or represented via the low-level method, based on empirically determined cutoffs, V_{cut}, for the predicted strength of pairwise couplings.

(2) When represented in local-mode coordinates, an additional distance-based screening can be applied. In the present case, this cutoff is necessarily applied at the low level of theory, in order to avoid the need for pre-screening at large distances. In order to generate the appropriate savings, the distance-based truncation is applied first to the low-level method; any remaining couplings are then used in the multilevel/pre-screening method in step (1). The windowed,[68] distance-based localization scheme[65] (analogous to Boys localization for molecular orbitals[110]), which maximizes the distance between mode centers and uses the same center-to-center values for distance truncation, was employed in the present analysis.

For clarity in nomenclature during the remainder of this analysis, we define the pre-screening method's potentials as

$$V^{(2)} = \sum_i V^{(1)}_{\text{target}}(q_i) + \sum_{\substack{i,j\in \\ \{\langle \Delta V^{(2)}_{ij,\text{low}} \rangle_{00} > V_{\text{cut}}\}}} \Delta V^{(2)}_{\text{target}}(q_i, q_j) \tag{3}$$

A multilevel method's potential (wherein low-level couplings are retained when they fall below V_{cut}) would analogously be defined as

$$V^{(2)} = \sum_i V^{(1)}_{\text{target}}(q_i) + \sum_{\substack{i,j\in \\ \{\langle \Delta V^{(2)}_{ij,\text{low}} \rangle_{00} \le V_{\text{cut}}\}}} \Delta V^{(2)}_{\text{low}}(q_i, q_j) + \sum_{\substack{i,j\in \\ \{\langle \Delta V^{(2)}_{ij,\text{low}} \rangle_{00} > V_{\text{cut}}\}}} \Delta V^{(2)}_{\text{target}}(q_i, q_j) \tag{4}$$

A distance-pre-screened method's potential, for which mode-pair couplings are retained when their mode center-to-center distances[65,67] r_{ij} fall below r_{cut} is defined as

$$V^{(2)} = \sum_i V^{(1)}_{\text{target}}(q_i) + \sum_{i,j\in\{r_{ij} \le r_{\text{cut}}\}} \Delta V^{(2)}_{\text{target}}(q_i, q_j) \tag{5}$$

And, finally, the targeted multilevel, distance-pre-screened method exhibits a potential defined as

$$V^{(2)} = \sum_i V^{(1)}_{\text{target}}(q_i) + \sum_{\substack{i,j\in \\ \{(r_{ij} \le r_{\text{cut}}) \text{ and } \\ \langle \Delta V^{(2)}_{ij,\text{low}} \rangle_{00} \le V_{\text{cut}}\}}} \Delta V^{(2)}_{\text{low}}(q_i, q_j) + \sum_{\substack{i,j\in \\ \{(r_{ij} \le r_{\text{cut}}) \text{ and } \\ \langle \Delta V^{(2)}_{ij,\text{low}} \rangle_{00} > V_{\text{cut}}\}}} \Delta V^{(2)}_{\text{target}}(q_i, q_j) \tag{6}$$

Before proceeding to the details of our test systems and the associated computations, some comment regarding step (2), above, is first warranted. Superficially, an acceleration of the low-level computations appears to be a rather modest improvement to existing multilevel methods. However, the central crux of the present investigation is that, if the multilevel pre-screening is sufficiently successful (and effectively local), it should render the high-level coupling computations linearly scaling with the number of vibrational modes (or atoms). If no locality was enforced for the low-level couplings, then they—with quadratic scaling for pairwise couplings, albeit with a smaller prefactor—would quickly become the computational bottleneck for systems of sufficient size. This somewhat paradoxical outcome motivates the combination with local-mode methods, wherein the low-level couplings also become linearly scaling due to the enforced distance cutoffs.

The guiding questions of the present investigation include the following:

Screening: To what extent, if any, can low-level pre-screening accelerate anharmonic simulations within local-mode coordinates? Are low-level couplings sufficiently accurate to adequately mimic screening by the target-level method?

Low-Level Recycling: Is recycling of low-level couplings an improvement over pre-screening alone, and can the use of this recyling approach yield more aggressive cutoffs at the target level of theory?

Local Modes: Are the necessary distance-based cutoffs used at the low level of theory similar to cutoffs observed in previous local-mode analyses? Does "pre-pre"-screening via distance sufficiently accelerate the low-level component of multilevel methods?

Convergence of VSCF ground-state energies and fundamental transitions ($\nu = 0 \rightarrow 1$) have been used as metrics for comparison. These values were computed as functions of coupling-energy and local-mode distance cutoffs and combinations thereof. Cutoffs were tested at a series of values, and results are plotted as the corresponding fraction of the number of target-level couplings retained (which will often yield unequally spaced data in the ensuing plots).

The VSCF calculations were performed in a basis set of 10 harmonic-oscillator functions with widths matched to the harmonic frequencies of each mode, which correspond to the square root of diagonal mass-weighted Hessian elements for local modes. Gauss−Hermite quadrature with 11 quadrature points was employed for all integrations. Sparser grids and/or multigrid approaches could potentially be used to accelerate these methods further, but consistent grids are used throughout in order to isolate local-mode and multilevel effects. Convergence of the iterative VSCF procedure was accelerated with the recently implemented vDIIS algorithm[111] to a tolerance of 10^{-6} E_h in the maximum value of the DIIS error vector across all modes, using a maximum of 4000 SCF cycles. Window-localized (500 cm^{-1} window) coordinates were used for all molecules. The target-level modes were used for both low- and target-level quadratures in order to avoid inconsistency of grids. Recent analyses[59] suggest that low-level mode displacements may suffice for this purpose, although the present investigation has proceeded under the assumption that target-level harmonic analyses would likely have been performed anyway for initial method screening and conformer relative energies, as applicable.

Selected test systems range from small molecules—ethylene, C_2H_4 [12 modes], and hexatriene, C_6H_8 [36 modes]—to the earlier-examined alanine dipeptide, $C_6N_2O_2H_{12}$ [60 modes].

https://doi.org/10.1021/acs.jctc.3c00589
J. Chem. Theory Comput. 2023, 19, 5572−5585

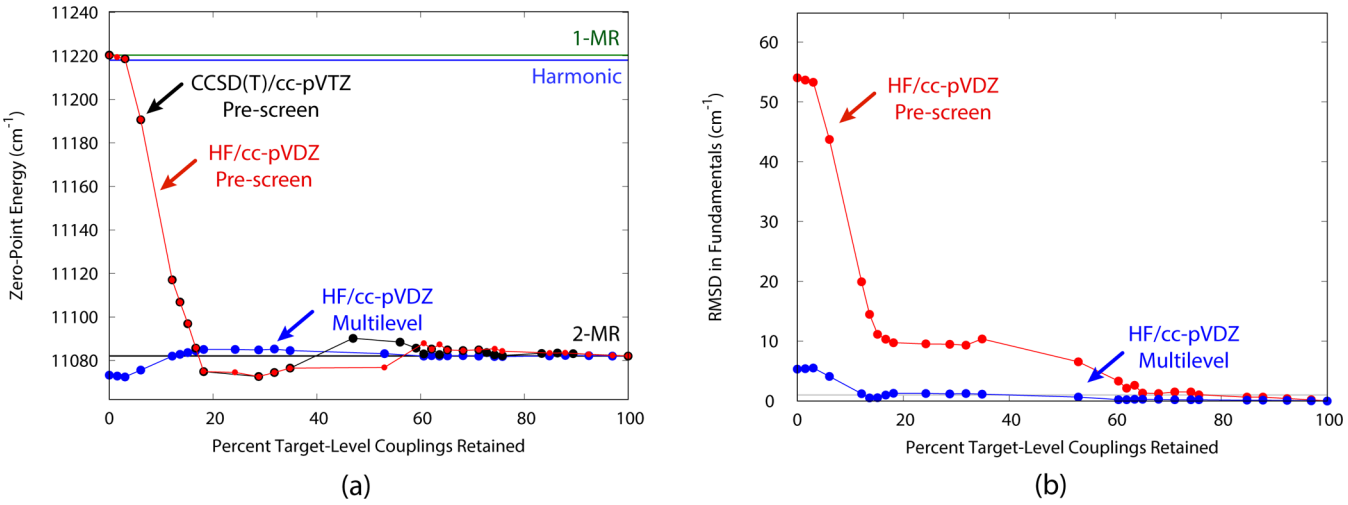

Figure 4. Pre-screening and multilevel 2-MR VSCF results for ethylene with the local-mode, CCSD(T)/cc-pVTZ method. (a) Zero-point energies as a function of the number of target-level couplings included, using pre-screening and multilevel (recycling) methods. (b) Root-mean-squared deviations (RMSDs) in fundamental transition energies as a function of target-level couplings included. The light gray line corresponds to a 1 cm^{-1} root-mean-squared deviations threshold for reference. The corresponding RMSD value for harmonic fundamentals is 104 cm^{-1}.

This variety of test cases is sufficiently large to explore the size dependence of the local, multilevel approach while still affording the reference untruncated calculations for comparison. For ethylene, the CCSD(T)/cc-pVTZ target method, within the frozen-core approximation, was combined with a series of low-level potentials, including CCSD, MP2, and HF with the cc-pVTZ, cc-pVDZ, and 6-31G basis sets. The target-level method for hexatriene was B3LYP/cc-pVTZ, using the pruned SG-3 exchange-correlation quadrature grid; its low-level pair was B3LYP/cc-pVDZ with the same grid. For Ala_2, an RI-MP2/cc-pVTZ target-level potential, within the frozen-core approximation, was combined with the RI-MP2/cc-pVDZ and HF/cc-pVDZ low-level potentials. All quantum chemistry computations were performed within the Q-Chem software package. Because of recently discovered problems with VSCF calculations and 2-MR potentials in cases of strong couplings,[57] 19 and 12 selected mode triples were included as a fixed background correction—with no multilevel or distance truncations—in the hexatriene and Ala_2 cases, respectively. This approach was employed merely to achieve VSCF convergence for all examined states while allowing for a targeted assessment of local, multilevel behavior specifically for the 2-MR portion of the potential. Analysis of multilevel and local effects in these 3- and higher-MR terms is reserved for a future investigation, although the need for such terms, even in the present test cases, suggests that such investigations are warranted. Because of the presence of terminal methyl rotors (which rectilinear 2-MR potentials are ill-suited to describe), the 4 lowest-frequency modes in Ala_2 were omitted in the VSCF calculation, again merely to achieve VSCF convergence. All ensuing statistical analyses properly account for the omission of these couplings.

RESULTS AND DISCUSSION

Ethylene. This first example provides the opportunity to explore the multilevel and pre-screening behavior in local modes, with the antecedent caveat that little distance dependence is anticipated in such a small molecule. For this reason, the multilevel behavior will be the primary focus for ethylene.

Results for the local-mode, 2-MR VSCF representation of ethylene's ground-state energy are depicted in Figure 4a. All reference values are depicted as fixed, horizontal lines in these figures. The reference CCSD(T)/cc-pVTZ data exhibits a slight blue shift upon inclusion of 1-MR anharmonicity; a subsequent 138 cm^{-1} red shift occurs upon inclusion of 2-MR coupling. Pre-screening by the target-level method alone (black data points) exhibits a rapid—although not monotonic—convergence toward the converged 2-MR value, with somewhat of a long tail after the initial drop from the limiting 1-MR value. Such results are included here only for comparison purposes, under the assumption that the PES computation is the (overwhelming) computational bottleneck when using *ab initio* potentials. Acceleration of the ensuing VSCF and correlated-mode calculations would also result from this target-level truncation if used in isolation.[96] The slight oscillations in this convergence behavior suggest that other coupling estimates may improve upon the current RMS definition. Such improvements could include the use of 1D anharmonic states in the coupling integration, maximum coupling elements among all basis functions coupled to the targeted state, noniterative VSCF estimates of a coupling's impact on the energy, perturbation theory estimates, definitions that account for resonance, or some combination of these approaches. These improvements are reserved for future analyses, as the present definition serves as a simple and transferable definition that exhibits sufficiently rapid convergence.

The HF/cc-pVDZ method provides reasonable estimates of the same 2-MR pre-screening (red data points in Figure 4a). (As a reminder to the reader, only target-level VSCF calculations are performed for each data point; the low-level pre-screening is simply used to determine which pairwise couplings are included at this target level.) Some slight deviations exist in the range of 35−55% retained couplings, but the overall convergence pattern is quite well reproduced by this much more economical method. Because of the small size of this molecule, nearly all of the couplings would need to be retained for sufficient accuracy, but the ability of the low-level method to reproduce this convergence behavior is the main metric of interest in this analysis. Interestingly, nearly all tested low-level methods,

https://doi.org/10.1021/acs.jctc.3c00589
J. Chem. Theory Comput. 2023, 19, 5572−5585

ranging from HF/6-31G to CCSD/cc-pVTZ, performed similarly. Plots analogous to Figure 4a for these alternative low-level methods are included in Figure S1 in the Supporting Information.

Given that the low-level methods yield two-mode couplings with accurate convergence patterns, their ability to replace the target-level couplings, rather than just pre-screen them, is worthy of investigation. Also in Figure 4a, recycling of these low-level couplings is examined with the same series of energy cutoffs (blue data points), again for the local-mode VSCF zero-point energy. Couplings above the selected cutoffs, as estimated by the low-level method, are retained at the target level of theory; 2-MR potentials for couplings below the cutoff are substituted by the low-level method's potential. Convergence in this case is notably more rapid. Even with low-level couplings alone (0% target couplings), the 2-MR VSCF is within 8.8 cm^{-1} of the full, target-level results. Although pre-screening required 91% of couplings in order to reach results within a wavenumber of cutoff-free values, the HF/cc-pVDZ pre-screening method—with recycling—required only 61% of target-level couplings.

Figure 4b presents analogous results for fundamental ($\nu = 0 \rightarrow 1$) transitions in ethylene. Shown are the root-mean-squared deviations (RMSD) of multilevel methods' transitions from target-level transitions in the absence of any pre-screening or recycling. The low-level pre-screening method is already a notable improvement over harmonic (RMSD: 104 cm^{-1}) or 1-MR (RMSD: 54 cm^{-1}) approaches upon inclusion of only a small fraction of mode pairs. However, the multilevel method with recycling of low-level couplings performs appreciably better. Inclusion of, at most, 53% of target-level couplings is required to reach sub-wavenumber fidelity with target-level results. This fraction corresponds to a coupling cutoff of V_{cut} = 25 cm^{-1}. Evidently, some of the nuanced quantum chemistry details also cancel in state-energy differences and make transition energies converge somewhat faster than specific state energies, at least for these types of simple fundamentals. Therefore, results for ethylene reaffirm that low-level pre-screening—when combined with re-use of the smaller-value, low-level couplings—can effectively approach target-level spectra with a small fraction of target-level couplings.

Hexatriene. For the hexatriene example, a simple combination of basis sets (cc-pVDZ/cc-pVTZ) was explored within the B3LYP density functional framework for multilevel purposes. Given the $O(N^4)$ scaling of SCF methods with respect to basis set size, this basis set change alone yields a 31-fold acceleration of the potential energy surface computations. This molecule, although still relatively small, is now large enough that the distance dependence of mode couplings can also be explored within the multilevel framework. All data for this molecule is presented in Figure 5.

The low-level pre-screening once again performs reasonably well. As shown in Figure 5a, pre-screening with this B3LYP/cc-pVDZ low level (red data points) closely—but not perfectly—mimics the behavior of the for-testing-purposes-only B3LYP/cc-pVTZ pre-screening method (black data points) for the zero-point energy of hexatriene. With pre-screening alone, sub-wavenumber fidelity with the reference ZPE is achieved at ≥74% of the included couplings (464 of 630 unique pairs).

The behavior of the multilevel method, which includes low-level recycling of omitted high-level couplings, is once again observed to be notably superior (blue data points in Figure 5a). When only low-level couplings are included, the error in the hexatriene ZPE is only −28 cm^{-1}. This value is a notable

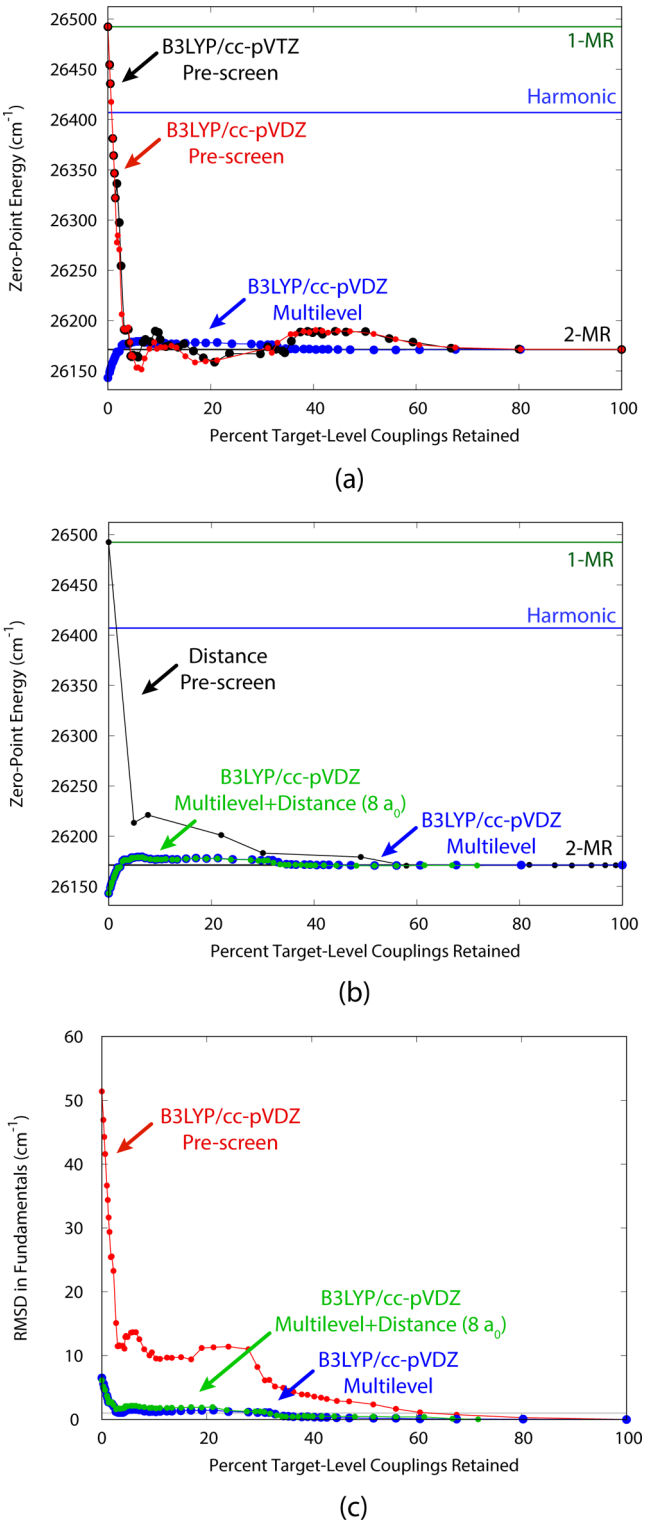

Figure 5. Pre-screening and multilevel 2-MR VSCF results for hexatriene with the local-mode, B3LYP/cc-pVTZ method. (a) Zero-point energies as a function of the number of target-level couplings included, using pre-screening and multilevel (recycling) methods. (b) Zero-point energies with distance-based cutoffs and multilevel methods with/without an 8 Bohr distance cutoff. (c) Root-mean-squared deviations in fundamental transition energies as a function of target-level couplings included. The light gray line corresponds to a 1 cm^{-1} RMSD threshold, for reference. The corresponding RMSD value for harmonic fundamentals is 89 cm^{-1}.

https://doi.org/10.1021/acs.jctc.3c00589
J. Chem. Theory Comput. 2023, 19, 5572−5585

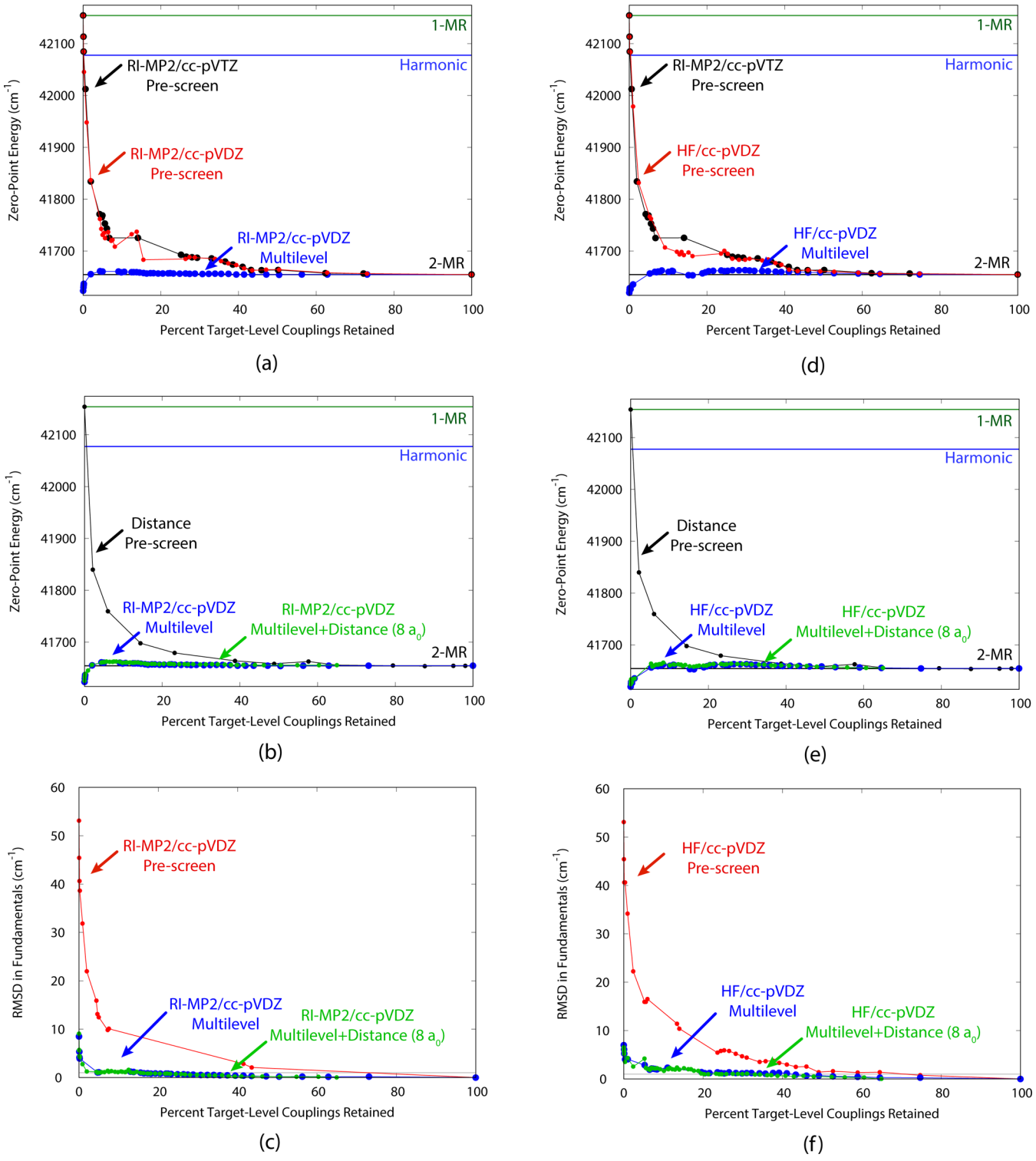

Figure 6. Pre-screening and multilevel 2-MR VSCF results for the alanine dipeptide with the local-mode, RI-MP2/cc-pVTZ method. (a−c) RI-MP2/cc-pVDZ low-level method. (d)−(f) HF/cc-pVDZ low-level method. (a, d) Zero-point energies as a function of the number of target-level couplings included, using pre-screening and multilevel (recycling) methods. (b, e) Zero-point energies with distance-based cutoffs and multilevel methods with/without an 8 Bohr distance cutoff. (c, f) Root-mean-squared deviations in fundamental transition energies as a function of target-level couplings included. The light gray line corresponds to a 1 cm^{-1} RMSD threshold, for reference. The corresponding RMSD value for harmonic fundamentals is 88 cm^{-1}.

improvement over both harmonic and 1-MR results, suggesting that the low-level couplings are at least qualitatively modeling the target-level couplings correctly. Upon inclusion of only a small handful of target-level couplings, this error improves further, and only 35% of target-level couplings (corresponding to a coupling cutoff of 15 cm^{-1}) are required to stably reach a sub-wavenumber error in the ZPE. If more aggressive truncations are desired by the user, the inclusion of only 11 of

https://doi.org/10.1021/acs.jctc.3c00589
J. Chem. Theory Comput. 2023, 19, 5572−5585

the 630 (1.7%) total target-level couplings yields an error of 2.3 cm^{-1}.

Although hexatriene is not a "large" molecule by almost any metric, it is sufficiently large to begin to assess the role of mode locality. In Figure 5b, the behavior of the 2-MR VSCF ground-state energy, with distance-based pre-screening applied, is depicted (black data points). The convergence based on distance alone is observed to roughly approximate the convergence of energy pre-screening (Figure 5a). The initial decay of the distance-based approach is somewhat slower, as a function of the number of included pairs, but it is also smoother and reaches the converged tail sooner than coupling-based screening. Using a standard[67,68] 8 Bohr cutoff in combination with the multilevel method yields results that are essentially indistinguishable from the multilevel results alone. In this approach, the low-level method is used to determine couplings to include at the target level, and only the low-level couplings inside the distance cutoff are retained at the low level. For hexatriene, 72% of the low-level couplings are retained at this rather conservative distance cutoff. But the method yields near-perfect fidelity with the multilevel results that were obtained in the absence of any distance cutoffs, suggesting that the removal of long-distance pairs bears little impact on the core multilevel effects.

Similar outcomes were observed for the fundamental transitions in hexatriene. The harmonic and 1-MR methods, at the target level, yield RMS errors in fundamentals of 89 and 51 cm^{-1}, respectively. The low-level pre-screening notably reduces these errors and achieves a sub-wavenumber RMSD by 64% of included couplings. The multilevel method (with recycling) reduces the errors further, and only 33% of target-level couplings are required for a converged, sub-wavenumber RMSD. Perhaps more significantly for larger systems, this multilevel method allows for an increase in the corresponding V_{cut} value from 2.5 to 16 cm^{-1}. The multilevel results with an additional 8 Bohr distance cutoff add some modest error (~0.4 cm^{-1}) at particularly aggressive cutoffs but converge to the 1 cm^{-1} RMSD error at the same number of target-level couplings.

Overall, this modestly sized molecule demonstrates that the multilevel method is an effective and efficient approach to yield target-level spectra at a fraction of the computational cost. The distance-based truncation of low-level couplings still yields sufficiently faithful representations of these multilevel results. Hexatriene is not yet large enough to allow for abundant reduction in the low-level cost, but it demonstrates that the distance-based cutoffs do not materially alter the overall behavior and that long-range, low-level couplings can be safely neglected.

Alanine Dipeptide. The Ala_2 case provides the opportunity to examine multilevel and distance behavior in a slightly larger molecule. The analysis for this case largely mirrors the hexatriene case, although results for multiple low-level methods (using an RI-MP2/cc-pVTZ target) are also compared here.

Results for the ground-state energy, using the RI-MP2/cc-pVDZ low-level method, are depicted in Figure 6a. The low-level pre-screening results once again match target-level pre-screening results across most of the mode-pair space, indicating that the coupling alignment depicted in Figure 3 does indeed yield sufficiently accurate pre-screening behavior. With RI-MP2/cc-pVDZ pre-screening alone, retention of 73% of the target-level mode couplings—corresponding to a coupling cutoff of 1 cm^{-1}—is required to yield a ZPE within a wavenumber of the cutoff-free value. When the low-level couplings are retained in the multilevel method, convergence is attained at far fewer target-level couplings. For Ala_2 and this methodology pairing, only 39% of target-level couplings are required in order to stably reach the same convergence threshold. This value is approximately the same as was observed in hexatriene, even though Ala_2 possesses almost twice as many vibrational modes. Given that Ala_2 is also more three-dimensional than the pseudo-1D hexatriene molecule, this outcome is reasonable.

The distance decay behavior in this larger molecule (Figure 6b) is both smoother and more monotonic than in the preceding examples. Single-wavenumber convergence of the ZPE is attained at the same 8 Bohr cutoff (65% of mode pairs, excluding mode pairs involving the four lowest-frequency modes) that was used in hexatriene, however. This cutoff, when combined with the multilevel method (RI-MP2/cc-pVDZ), is once again nearly indistinguishable from multilevel-only results and yields the same distance-based 35% acceleration of the low-level method.

Fundamental transitions in Ala_2 (Figure 6c) are also well reproduced by this combination. Low-level pre-screening alone is already a notable improvement over harmonic spectra (RMSD: 88 cm^{-1}). The multilevel method reaches the arbitrary 1 cm^{-1} error threshold by only 4.7% of target-level mode couplings, and it remains stable within this error by 16% of couplings (V_{cut} = 30 cm^{-1}). The approximate transferability of the V_{cut} value across the test systems in this work (15−30 cm^{-1}) is an encouraging outcome suggesting that a suitably transferable cutoff may exist that would not require incremental convergence tests in practice during a multilevel calculation. The ensuing multilevel-plus-distance approach (8 Bohr) converges at the same number of target-level couplings but can also omit 35% of the low-level pairings prior to pre-screening. As a tangible example, the intramolecular, H-bonded amide N−H fundamental stretch frequency is 3543.57 cm^{-1} with both the target-level and multilevel-plus-distance methods at the cutoffs described above. (The absolute transition frequencies will shift upon inclusion of mode-correlation effects, especially for local modes;[41,82] however, the consistency of the reference local-mode VSCF transitions is the metric of interest in the present analysis.)

Nearly all of the qualitative conclusions remain intact when using an HF/cc-pVDZ low-level potential instead, as shown in Figure 6d−f, although some tradeoff in low-level efficiency and high-level screening is observed. The multilevel method again converges rapidly—at 43% of couplings, after beginning at a 7 cm^{-1} error for fundamentals—and the addition of a distance cutoff (at 8 Bohr) yields convergence at the same value. Whether this low-level method could be extended "lower" to semi-empirical or other potentials will likely be system-dependent. The same modest tradeoff observed here may apply to these alternative approaches, although efficient methods to pre-screen[79] may temper the need for such considerations.

One possible hiccup in the use of these multilevel approaches is a scenario in which the removal of certain couplings—especially at particularly aggressive truncation values—induces poor or incomplete convergence of the VSCF procedure. Indeed, this case was observed at some truncation values for Ala_2 and explains some of the gaps in the convergence data of Figure 6. Although the details of this scenario have not yet been investigated in detail, we suspect that some imbalance of couplings yields regions of negative potentials[57] in these cases and induces poor VSCF convergence, at least with 2-MR

https://doi.org/10.1021/acs.jctc.3c00589
J. Chem. Theory Comput. 2023, 19, 5572−5585

potentials. Empirically, the unconverged VSCF values were observed to be quite reasonable, compared to the values at neighboring truncation values. The states are likely not far from convergence, and further improvements to VSCF convergence algorithms may suffice to attain converged results. Perhaps more meaningfully, 3- and 4-MR potentials could also likely help avoid these situations, and the multilevel methods could also be extended to this higher-accuracy regime.

As indicated in Figure 3, the cc-pVDZ basis set yields RI-MP2 calculations that are ∼14 times faster than the cc-pVTZ target-level calculations. (For anharmonic vibrational simulations, the RI-MP2 force[112,113] would be computed in order to yield relaxed dipole moments.) Using the multilevel-plus-distance, local-mode method would yield a 4.8-fold acceleration over target-level results. Switching to the HF/cc-pVDZ low-level method would increase this value to a 5.9-fold acceleration, although the distance-based truncation impacts this latter value to a smaller degree. These figures correspond to our best real-world estimates of the accelerations that should be anticipated for local-mode, multilevel methods when using 2-MR potentials for small biomolecules. These relative savings should only increase for larger molecules/complexes and higher-order *n*-MR potentials.

Scaling and Outlook. The three test systems in this analysis demonstrated that the multilevel (with recycling) method is an effective route to obtain target-level results with considerable reduction in the requisite number of target-level couplings. In a local-mode representation, the number of substantive, retained couplings must scale linearly in the number of vibrational modes. This approximate $O(N^2) \rightarrow O(N)$ reduction in the number of coupled mode pairs is the main outcome of the multilevel approach, and given that the target-level couplings originally dominated the cost of the computation, this acceleration is the main source of the computational efficiency of this method.

However, this scenario also leads to a somewhat paradoxical conclusion for larger molecules: namely, the quadratic scaling $\left[\frac{N(N-1)}{2}\right]$ of the low-level method renders it the cost-dominant component for molecules larger than the ones considered here. When the fractional reduction in cost of a single low-level quantum chemistry calculation is exceeded by the fractional reduction in requisite target-level couplings, the low-level method would dominate the cost of the calculation. In the alanine dipeptide case, for example, a 6-fold reduction in target-level (RI-MP2/cc-pVTZ) couplings was paired with a 14-fold reduction in PES evaluation at the low-level (RI-MP2/cc-pVDZ). If the former remained approximately constant, only an approximate doubling of the system size would be required to make the two components competitive (without a distance cutoff). The fraction of target-level couplings removed by pre-screening likely also increases with system size, so this estimate is rather crude. But it demonstrates that small polypeptides would nonetheless likely reach the size regime where this crossover would occur. Application of local-mode, distance-based cutoffs for these low-level couplings, therefore, is necessary in order to tackle this burgeoning computational bottleneck as the system size increases. Given that the examples presented herein demonstrated good fidelity between multilevel and multilevel-plus-distance, local-mode methods, this approach appears to be an appropriate strategy for larger molecules and complexes.

CONCLUSIONS

Simulations of anharmonic vibrational motion provide a critical conduit between modern spectroscopy experiments and physical/chemical insight. The need to compute mode-coupling potential energy surfaces poses prohibitive computational cost challenges for many molecules of current (and future) interest, however, especially when spectroscopically accurate, *ab initio* potentials are employed. The present analysis has assessed the suitability of combining local-mode methods with multilevel approaches. Provided that the low-level couplings are "recycled"—because they would necessarily be computed anyway—this approach was determined to be particularly effective and yielded sub-wavenumber errors with approximately 5-fold accelerations for spectroscopically relevant potentials on a small biomolecule.

This analysis specifically focused on the efficacy of the combined local-mode, multilevel methodology for 2-MR potentials and VSCF calculations. Because the strongest couplings exist at short range in a local-mode representation, these relative multilevel accelerations are anticipated to improve for larger systems. Given known scaling relationships and previous examinations of the local-mode approach, the savings for the low-level method—which should become cost-dominant for systems not much larger than those examined herein—should also benefit from distance-based truncations. The behavior for correlated-mode simulations (VCI and similar) may differ somewhat from the conclusions observed here, and additional investigation of this behavior is warranted. Given the tight convergence thresholds and conservative distance cutoffs employed herein, few problems are anticipated. Small-coupling resonant states could perhaps pose challenges to naïve cutoff-based algorithms, but sufficiently accurate pre-screening approaches should capture these effects, as well.

Furthermore, these computational cost estimates are lower bounds for the accelerations anticipated for higher-order terms in the *n*-MR. As was previously demonstrated for local-mode methods,[68] the cutoffs can be more aggressive at higher orders, and the fraction of requisite mode triples falling within a given distance cutoff is substantially lower. Accordingly, considerable motivation exists to pursue 3- and 4-MR potentials within the same framework in future investigations, especially since these often numerically small terms can also rectify many known qualitative failures[57] in VSCF simulations of larger systems. If this combination of techniques allows for performing high-order *n*-MR expansions with well-justified coupling and distance cutoffs, then the simulation community would have a means of accurately and efficiently targeting only the important anharmonic couplings without undue overhead to predict such couplings. This method, therefore, may be a route toward stable, reliable simulations of biomolecules and larger clusters. It will not obviate the need for thermodynamic sampling or address the presence of perhaps hundreds or thousands of thermally accessible conformers. But it may enable routine spectral simulations of molecules within each of these minima.

ASSOCIATED CONTENT

Supporting Information

The Supporting Information is available free of charge at https://pubs.acs.org/doi/10.1021/acs.jctc.3c00589.

Comparison of pre-screening behavior across low-level methods for ethylene (Figure S1) (PDF)

https://doi.org/10.1021/acs.jctc.3c00589
J. Chem. Theory Comput. 2023, 19, 5572−5585

AUTHOR INFORMATION

Corresponding Author

Ryan P. Steele − *Department of Chemistry and Henry Eyring Center for Theoretical Chemistry, University of Utah, Salt Lake City, Utah 84112, United States;* orcid.org/0000-0002-3292-9805; Email: ryan.steele@utah.edu

Authors

Asylbek A. Zhanserkeev − *Department of Chemistry and Henry Eyring Center for Theoretical Chemistry, University of Utah, Salt Lake City, Utah 84112, United States*

Emily L. Yang − *Department of Chemistry and Henry Eyring Center for Theoretical Chemistry, University of Utah, Salt Lake City, Utah 84112, United States;* orcid.org/0009-0005-9839-964X

Complete contact information is available at: https://pubs.acs.org/10.1021/acs.jctc.3c00589

Notes

The authors declare no competing financial interest.

ACKNOWLEDGMENTS

The authors acknowledge funding from the U.S. National Science Foundation under Grant CHE-2102309. The support and resources of the Center for High-Performance Computing at the University of Utah are gratefully acknowledged. This work also used the Extreme Science and Engineering Discovery Environment (XSEDE), which is supported by National Science Foundation grant no. ACI-1548562.

REFERENCES

(1) Duong, C. H.; Yang, N.; Johnson, M. A.; DiRisio, R. J.; McCoy, A. B.; Yu, Q.; Bowman, J. M. Disentangling the Complex Vibrational Mechanics of the Protonated Water Trimer by Rational Control of Its Hydrogen Bonds. *J. Phys. Chem. A* **2019**, *123*, 7965−7972.

(2) Guasco, T. L.; Johnson, M. A. Applications of Lasers and Mass Spectrometry in Molecular Spectroscopy and Molecular Structure Determination. In *Emerging Trends in Chemical Applications of Lasers*, ACS Symposium Series; American Chemical Society, 2021; Vol. *1398*, pp 277−306.

(3) Leavitt, C. M.; Wolk, A. B.; Fournier, J. A.; Kamrath, M. Z.; Garand, E.; Van Stipdonk, M. J.; Johnson, M. A. Isomer-Specific IR−IR Double Resonance Spectroscopy of D_2-Tagged Protonated Dipeptides Prepared in a Cryogenic Ion Trap. *J. Phys. Chem. Lett.* **2012**, *3*, 1099−1105.

(4) McCoy, A. B.; Guasco, T. L.; Leavitt, C. M.; Olesen, S. G.; Johnson, M. A. Vibrational Manifestations of Strong Non-Condon Effects in the $H_3O^+{\cdot}X_3$ (X = Ar, N_2, CH_4, H_2O) Complexes: A Possible Explanation for the Intensity in the "Association Band" in the Vibrational Spectrum of Water. *Phys. Chem. Chem. Phys.* **2012**, *14*, 7205−7214.

(5) Talbot, J. J.; Yang, N.; Huang, M.; Duong, C. H.; McCoy, A. B.; Steele, R. P.; Johnson, M. A. Spectroscopic Signatures of Mode-Dependent Tunnel Splitting in the Iodide−Water Binary Complex. *J. Phys. Chem. A* **2020**, *124*, 2991−3001.

(6) Wolk, A. B.; Leavitt, C. M.; Garand, E.; Johnson, M. A. Cryogenic Ion Chemistry and Spectroscopy. *Acc. Chem. Res.* **2014**, *47*, 202−210.

(7) Yang, N.; Khuu, T.; Mitra, S.; Duong, C. H.; Johnson, M. A.; DiRisio, R. J.; McCoy, A. B.; Miliordos, E.; Xantheas, S. S. Isolating the Contributions of Specific Network Sites to the Diffuse Vibrational Spectrum of Interfacial Water with Isotopomer-Selective Spectroscopy of Cold Clusters. *J. Phys. Chem. A* **2020**, *124*, 10393−10406.

(8) Zeng, H. J.; Johnson, M. A. Demystifying the Diffuse Vibrational Spectrum of Aqueous Protons through Cold Cluster Spectroscopy. *Annu. Rev. Phys. Chem.* **2021**, *72*, 667−691.

(9) Polfer, N. C. Infrared Multiple Photon Dissociation Spectroscopy of Trapped Ions. *Chem. Soc. Rev.* **2011**, *40*, 2211−2221.

(10) Garand, E. Spectroscopy of Reactive Complexes and Solvated Clusters: A Bottom-up Approach Using Cryogenic Ion Traps. *J. Phys. Chem. A* **2018**, *122*, 6479−6490.

(11) Marsh, B. M.; Voss, J. M.; Garand, E. A Dual Cryogenic Ion Trap Spectrometer for the Formation and Characterization of Solvated Ionic Clusters. *J. Chem. Phys.* **2015**, *143*, No. 204201.

(12) Armentrout, P. B.; Stevenson, B. C.; Ghiassee, M.; Boles, G. C.; Berden, G.; Oomens, J. Infrared Multiple-Photon Dissociation Spectroscopy of Cationized Glycine: Effects of Alkali Metal Cation Size on Gas-Phase Conformation. *Phys. Chem. Chem. Phys.* **2022**, *24*, 22950−22959.

(13) Martens, J.; Berden, G.; Gebhardt, C. R.; Oomens, J. Infrared Ion Spectroscopy in a Modified Quadrupole Ion Trap Mass Spectrometer at the Felix Free Electron Laser Laboratory. *Rev. Sci. Instrum.* **2016**, *87*, No. 103108.

(14) Vendrell, O.; Gatti, F.; Meyer, H.-D. Dynamics and Infrared Spectroscopy of the Protonated Water Dimer. *Angew. Chem., Int. Ed.* **2007**, *46*, 6918−6921.

(15) Schröder, M.; Meyer, H.-D. Calculation of the Vibrational Excited States of Malonaldehyde and Their Tunneling Splittings with the Multi-Configuration Time-Dependent Hartree Method. *J. Chem. Phys.* **2014**, *141*, No. 034116.

(16) Schröder, M.; Gatti, F.; Lauvergnat, D.; Meyer, H.-D.; Vendrell, O. The Coupling of the Hydrated Proton to Its First Solvation Shell. *Nat. Commun.* **2022**, *13*, No. 6170.

(17) Carrington, T., Jr.; Wang, X.-G. Computing Ro-Vibrational Spectra of Van Der Waals Molecules. *Wiley Interdiscip. Rev.: Comput. Mol. Sci.* **2011**, *1*, 952−963.

(18) Carrington, T., Jr. Perspective: Computing (Ro-)Vibrational Spectra of Molecules with More Than Four Atoms. *J. Chem. Phys.* **2017**, *146*, No. 120902.

(19) Felker, P. M.; Bačić, Z. Intermolecular Vibrational States of HF Trimer from Rigorous Nine-Dimensional Quantum Calculations: Strong Coupling between Intermolecular Bending and Stretching Vibrations and the Importance of the Three-Body Interactions. *J. Chem. Phys.* **2022**, *157*, No. 194103.

(20) Felker, P. M.; Bačić, Z. Noncovalently Bound Molecular Complexes Beyond Diatom−Diatom Systems: Full-Dimensional, Fully Coupled Quantum Calculations of Rovibrational States. *Phys. Chem. Chem. Phys.* **2022**, *24*, 24655−24676.

(21) Carter, S.; Bowman, J. M.; Handy, N. C. Extensions and Tests of "Multimode": A Code to Obtain Accurate Vibration/Rotation Energies of Many-Mode Molecules. *Theor. Chem. Acc.* **1998**, *100*, 191−198.

(22) Yu, Q.; Qu, C.; Houston, P. L.; Conte, R.; Nandi, A.; Bowman, J. M. Multimode, the n-Mode Representation of the Potential and Illustrations to IR Spectra of Glycine and Two Protonated Water Clusters. In *Vibrational Dynamics of Molecules*; World Scientific, 2021; pp 296−339.

(23) Carrington, T., Jr Using Iterative Methods to Compute Vibrational Spectra. In *Handbook of High-Resolution Spectroscopy*; John Wiley & Sons, 2011.

(24) Bowman, J. M. Self-Consistent Field Energies and Wavefunctions for Coupled Oscillators. *J. Chem. Phys.* **1978**, *68*, 608−610.

(25) Christoffel, K. M.; Bowman, J. M. Investigations of Self-Consistent Field, SCF CI and Virtual State Configuration Interaction Vibrational Energies for a Model Three-Mode System. *Chem. Phys. Lett.* **1982**, *85*, 220−224.

(26) Bowman, J. M. The Self-Consistent-Field Approach to Polyatomic Vibrations. *Acc. Chem. Res.* **1986**, *19*, 202−208.

(27) Wierzbicki, A.; Bowman, J. M. Self-Consistent Field Investigation of Vibrations of Atomic Adsorbates. *J. Chem. Phys.* **1987**, *87*, 2363−2369.

(28) Carter, S.; Culik, S. J.; Bowman, J. M. Vibrational Self-Consistent Field Method for Many-Mode Systems: A New Approach and Application to the Vibrations of CO Adsorbed on Cu(100). *J. Chem. Phys.* **1997**, *107*, 10458−10469.

(29) Hirata, S.; Keçeli, M.; Yagi, K. First-Principles Theories for Anharmonic Lattice Vibrations. *J. Chem. Phys.* **2010**, *133*, No. 034109.
(30) Keçeli, M.; Hirata, S. Size-Extensive Vibrational Self-Consistent Field Method. *J. Chem. Phys.* **2011**, *135*, No. 134108.
(31) Christiansen, O. A Second Quantization Formulation of Multimode Dynamics. *J. Chem. Phys.* **2004**, *120*, 2140−2148.
(32) Christiansen, O. Selected New Developments in Vibrational Structure Theory: Potential Construction and Vibrational Wave Function Calculations. *Phys. Chem. Chem. Phys.* **2012**, *14*, 6672−6687.
(33) Erba, A.; Maul, J.; Ferrabone, M.; Dovesi, R.; Rerat, M.; Carbonniere, P. Anharmonic Vibrational States of Solids from DFT Calculations. Part II: Implementation of the VSCF and VCI Methods. *J. Chem. Theory Comput.* **2019**, *15*, 3766−3777.
(34) Roy, T. K.; Gerber, R. B. Vibrational Self-Consistent Field Calculations for Spectroscopy of Biological Molecules: New Algorithmic Developments and Applications. *Phys. Chem. Chem. Phys.* **2013**, *15*, 9468−9492.
(35) Roy, T. K.; Sharma, R.; Gerber, R. B. First-Principles Anharmonic Quantum Calculations for Peptide Spectroscopy: VSCF Calculations and Comparison with Experiments. *Phys. Chem. Chem. Phys.* **2016**, *18*, 1607−1614.
(36) Gerber, R. B.; Chaban, G. M.; Brauer, B.; Miller, Y. *Theory and Applications of Computational Chemistry: The First 40 Years*; Elsevier, 2005; pp 165−193.
(37) Jung, J. O.; Gerber, R. B. Vibrational Wave Functions and Spectroscopy of $(H_2O)_n$, n = 2,3,4,5: Vibrational Self-Consistent Field with Correlation Corrections. *J. Chem. Phys.* **1996**, *105*, 10332−10348.
(38) Matsunaga, N.; Chaban, G. M.; Gerber, R. B. Degenerate Perturbation Theory Corrections for the Vibrational Self-Consistent Field Approximation: Method and Applications. *J. Chem. Phys.* **2002**, *117*, 3541−3547.
(39) Mathea, T.; Rauhut, G. Advances in Vibrational Configuration Interaction Theory—Part 1: Efficient Calculation of Vibrational Angular Momentum Terms. *J. Comput. Chem.* **2021**, *42*, 2321−2333.
(40) Mathea, T.; Petrenko, T.; Rauhut, G. Advances in Vibrational Configuration Interaction Theory-Part 2: Fast Screening of the Correlation Space. *J. Comput. Chem.* **2022**, *43*, 6−18.
(41) Panek, P. T.; Hoeske, A. A.; Jacob, C. R. On the Choice of Coordinates in Anharmonic Theoretical Vibrational Spectroscopy: Harmonic vs. Anharmonic Coupling in Vibrational Configuration Interaction. *J. Chem. Phys.* **2019**, *150*, No. 054107.
(42) Christiansen, O. Vibrational Coupled Cluster Theory. *J. Chem. Phys.* **2004**, *120*, 2149−2159.
(43) Godtliebsen, I. H.; Thomsen, B.; Christiansen, O. Tensor Decomposition and Vibrational Coupled Cluster Theory. *J. Phys. Chem. A* **2013**, *117*, 7267−7279.
(44) König, C.; Christiansen, O. Automatic Determination of Important Mode−Mode Correlations in Many-Mode Vibrational Wave Functions. *J. Chem. Phys.* **2015**, *142*, No. 144115.
(45) Franke, P. R.; Stanton, J. F.; Douberly, G. E. How to VPT2: Accurate and Intuitive Simulations of CH Stretching Infrared Spectra Using VPT2+K with Large Effective Hamiltonian Resonance Treatments. *J. Phys. Chem. A* **2021**, *125*, 1301−1324.
(46) Ramakrishnan, R.; Rauhut, G. Semi-Quartic Force Fields Retrieved from Multi-Mode Expansions: Accuracy, Scaling Behavior, and Approximations. *J. Chem. Phys.* **2015**, *142*, No. 154118.
(47) Lin, C. Y.; Gilbert, A. T. B.; Gill, P. M. W. Calculating Molecular Vibrational Spectra Beyond the Harmonic Approximation. *Theor. Chem. Acc.* **2008**, *120*, 23−35.
(48) Roy, T. K. Performance of Vibrational Self-Consistent Field Theory for Accurate Potential Energy Surfaces: Fundamentals, Excited States, and Intensities. *J. Phys. Chem. A* **2022**, *126*, 608−622.
(49) Roy, T. K.; Carrington, T., Jr; Gerber, R. B. Approximate First-Principles Anharmonic Calculations of Polyatomic Spectra Using MP2 and B3LYP Potentials: Comparisons with Experiment. *J. Phys. Chem. A* **2014**, *118*, 6730−6739.
(50) Sibert, E. L. Modeling Anharmonic Effects in the Vibrational Spectra of High-Frequency Modes. *Annu. Rev. Phys. Chem.* **2023**, *74*, 219−244.
(51) Saparbaev, E.; Aladinskaia, V.; Zviagin, A.; Boyarkin, O. V. Microhydration of Biomolecules: Revealing the Native Structures by Cold Ion IR Spectroscopy. *J. Phys. Chem. Lett.* **2021**, *12*, 907−911.
(52) Saparbaev, E.; Yamaletdinov, R.; Boyarkin, O. V. Identification of Isomeric Lipids by UV Spectroscopy of Noncovalent Complexes with Aromatic Molecules. *Anal. Chem.* **2021**, *93*, 12822−12826.
(53) Saparbaev, E.; Zviagin, A.; Boyarkin, O. V. Identification of Isomeric Biomolecules by Infrared Spectroscopy of Solvent-Tagged Ions. *Anal. Chem.* **2022**, *94*, 9514−9518.
(54) Zviagin, A.; Kopysov, V.; Nagornova, N. S.; Boyarkin, O. V. Tracking Local and Global Structural Changes in a Protein by Cold Ion Spectroscopy. *Phys. Chem. Chem. Phys.* **2022**, *24*, 8158−8165.
(55) Pellegrinelli, R. P.; Yue, L.; Carrascosa, E.; Ben Faleh, A.; Warnke, S.; Bansal, P.; Rizzo, T. R. A New Strategy Coupling Ion-Mobility-Selective CID and Cryogenic IR Spectroscopy to Identify Glycan Anomers. *J. Am. Soc. Mass Spectrom.* **2022**, *33*, 859−864.
(56) Bansal, P.; Ben Faleh, A.; Warnke, S.; Rizzo, T. R. Multistage Ion Mobility Spectrometry Combined with Infrared Spectroscopy for Glycan Analysis. *J. Am. Soc. Mass Spectrom.* **2023**, *34*, 695−700.
(57) Yang, E. L.; Talbot, J. J.; Spencer, R. J.; Steele, R. P. Pitfalls in the n-Mode Representation of Vibrational Potentials. *J. Chem. Phys.* **2023**, (Under review, submitted 31 May 2023).
(58) Steen, N. M.; Byrne, G. D.; Gelbard, E. M. Gaussian Quadratures for the Integrals $\exp(-x^2)f(x)$. *Math. Comput.* **1969**, *23*, 661−671.
(59) Yagi, K.; Hirata, S.; Hirao, K. Multiresolution Potential Energy Surfaces for Vibrational State Calculations. *Theor. Chem. Acc.* **2007**, *118*, 681−691.
(60) Sparta, M.; Høyvik, I.-M.; Toffoli, D.; Christiansen, O. Potential Energy Surfaces for Vibrational Structure Calculations from a Multiresolution Adaptive Density-Guided Approach: Implementation and Test Calculations. *J. Phys. Chem. A* **2009**, *113*, 8712−8723.
(61) Carter, S.; Bowman, J. M.; Braams, B. J. On Using Low-Order Hermite Interpolation in 'Direct Dynamics' Calculations of Vibrational Energies Using the Code 'Multimode'. *Chem. Phys. Lett.* **2001**, *342*, 636−642.
(62) Carter, S.; Handy, N. C. On the Representation of Potential Energy Surfaces of Polyatomic Molecules in Normal Coordinates. *Chem. Phys. Lett.* **2002**, *352*, 1−7.
(63) Avila, G.; Carrington, T., Jr. Solving the Vibrational Schrödinger Equation Using Bases Pruned to Include Strongly Coupled Functions and Compatible Quadratures. *J. Chem. Phys.* **2012**, *137*, No. 174108.
(64) Strobusch, D.; Scheurer, C. Adaptive Sparse Grid Expansions of the Vibrational Hamiltonian. *J. Chem. Phys.* **2014**, *140*, No. 034107.
(65) Jacob, C. R.; Reiher, M. Localizing Normal Modes in Large Molecules. *J. Chem. Phys.* **2009**, *130*, No. 084106.
(66) Weymuth, T.; Jacob, C. R.; Reiher, M. A Local-Mode Model for Understanding the Dependence of the Extended Amide III Vibrations on Protein Secondary Structure. *J. Phys. Chem. B* **2010**, *114*, 10649−10660.
(67) Cheng, X.; Steele, R. P. Efficient Anharmonic Vibrational Spectroscopy for Large Molecules Using Local-Mode Coordinates. *J. Chem. Phys.* **2014**, *141*, No. 104105.
(68) Cheng, X.; Talbot, J. J.; Steele, R. P. Tuning Vibrational Mode Localization with Frequency Windowing. *J. Chem. Phys.* **2016**, *145*, No. 124112.
(69) Panek, P. T.; Jacob, C. R. Efficient Calculation of Anharmonic Vibrational Spectra of Large Molecules with Localized Modes. *ChemPhysChem* **2014**, *15*, 3365−3377.
(70) Panek, P. T.; Jacob, C. R. On the Benefits of Localized Modes in Anharmonic Vibrational Calculations for Small Molecules. *J. Chem. Phys.* **2016**, *144*, No. 164111.
(71) Yagi, K.; Keçeli, M.; Hirata, S. Optimized Coordinates for Anharmonic Vibrational Structure Theories. *J. Chem. Phys.* **2012**, *137*, No. 204118.
(72) Thompson, T. C.; Truhlar, D. G. Optimization of Vibrational Coordinates, with an Application to the Water Molecule. *J. Chem. Phys.* **1982**, *77*, 3031−3035.

https://doi.org/10.1021/acs.jctc.3c00589
J. Chem. Theory Comput. 2023, 19, 5572−5585

(73) König, C.; Christiansen, O. Linear-Scaling Generation of Potential Energy Surfaces Using a Double Incremental Expansion. *J. Chem. Phys.* **2016**, *145*, No. 064105.
(74) Madsen, D.; Christiansen, O.; König, C. Anharmonic Vibrational Spectra from Double Incremental Potential Energy and Dipole Surfaces. *Phys. Chem. Chem. Phys.* **2018**, *20*, 3445−3456.
(75) Tabor, D. P.; Hewett, D. M.; Bocklitz, S.; Korn, J. A.; Tomaine, A. J.; Ghosh, A. K.; Zwier, T. S.; Sibert, E. L., III. Anharmonic Modeling of the Conformation-Specific IR Spectra of Ethyl, n-Propyl, and n-Butylbenzene. *J. Chem. Phys.* **2016**, *144*, No. 224310.
(76) Bernath, P. F.; Sibert III, E. L. Cyclohexane Vibrations: High-Resolution Spectra and Anharmonic Local Mode Calculations. *J. Phys. Chem. A* **2020**, *124*, 9991−10000.
(77) Benoit, D. M. Fast Vibrational Self-Consistent Field Calculations through a Reduced Mode−Mode Coupling Scheme. *J. Chem. Phys.* **2004**, *120*, 562−573.
(78) Bounouar, M.; Scheurer, C. Reducing the Vibrational Coupling Network in N-Methylacetamide as a Model for Ab Initio Infrared Spectra Computations of Peptides. *Chem. Phys.* **2006**, *323*, 87−101.
(79) Ziegler, B.; Rauhut, G. Localized Normal Coordinates in Accurate Vibrational Structure Calculations: Benchmarks for Small Molecules. *J. Chem. Theory Comput.* **2019**, *15*, 4187−4196.
(80) König, C.; Christiansen, O. Automatic Determination of Important Mode−Mode Correlations in Many-Mode Vibrational Wave Functions. *J. Chem. Phys.* **2015**, *142*, No. 144115.
(81) Seidler, P.; Kaga, T.; Yagi, K.; Christiansen, O.; Hirao, K. On the Coupling Strength in Potential Energy Surfaces for Vibrational Calculations. *Chem. Phys. Lett.* **2009**, *483*, 138−142.
(82) Hanson-Heine, M. W. D. Examining the Impact of Harmonic Correlation on Vibrational Frequencies Calculated in Localized Coordinates. *J. Chem. Phys.* **2015**, *143*, No. 164104.
(83) Hanson-Heine, M. W. D. Intermediate Vibrational Coordinate Localization with Harmonic Coupling Constraints. *J. Chem. Phys.* **2016**, *144*, No. 204116.
(84) Hanson-Heine, M. W. D. Reduced Basis Set Dependence in Anharmonic Frequency Calculations Involving Localized Coordinates. *J. Chem. Theory Comput.* **2018**, *14*, 1277−1285.
(85) Kuenzer, U.; Klotz, M.; Hofer, T. S. Probing Vibrational Coupling Via a Grid-Based Quantum Approach-an Efficient Strategy for Accurate Calculations of Localized Normal Modes in Solid-State Systems. *J. Comput. Chem.* **2018**, *39*, 2196−2209.
(86) Molina, A.; Smereka, P.; Zimmerman, P. M. Exploring the Relationship between Vibrational Mode Locality and Coupling Using Constrained Optimization. *J. Chem. Phys.* **2016**, *144*, No. 124111.
(87) Bürger, H.; Ma, S.; Breidung, J.; Thiel, W. AbInitio Calculations and High Resolution Infrared Investigation on XeF_4. *J. Chem. Phys.* **1996**, *104*, 4945−4953.
(88) Bürger, H.; Kuna, R.; Ma, S.; Breidung, J.; Thiel, W. The Vibrational Spectra of Krypton and Xenon Difluoride: High-Resolution Infrared Studies and Ab Initio Calculations. *J. Chem. Phys.* **1994**, *101*, 1−14.
(89) Boese, A. D.; Martin, J. M. L. Vibrational Spectra of the Azabenzenes Revisited: Anharmonic Force Fields. *J. Phys. Chem. A* **2004**, *108*, 3085−3096.
(90) Begue, D.; Carbonniere, P.; Pouchan, C. Calculations of Vibrational Energy Levels by Using a Hybrid Ab Initio and DFT Quartic Force Field: Application to Acetonitrile. *J. Phys. Chem. A* **2005**, *109*, 4611−4616.
(91) Lutz, O. M. D.; Rode, B. M.; Bonn, G. K.; Huck, C. W. The Impact of Highly Correlated Potential Energy Surfaces on the Anharmonically Corrected IR Spectrum of Acetonitrile. *Spectrochim. Acta, Part A* **2014**, *131*, 545−555.
(92) Rauhut, G. Efficient Calculation of Potential Energy Surfaces for the Generation of Vibrational Wave Functions. *J. Chem. Phys.* **2004**, *121*, 9313−9322.
(93) Tan, J. A.; Kuo, J.-L. Multilevel Approach for Direct VSCF/VCI Multimode Calculations with Applications to Large "Zundel" Cations. *J. Chem. Theory Comput.* **2018**, *14*, 6405−6416.
(94) Respondek, I.; Benoit, D. M. Fast Degenerate Correlation-Corrected Vibrational Self-Consistent Field Calculations of the Vibrational Spectrum of 4-Mercaptopyridine. *J. Chem. Phys.* **2009**, *131*, No. 054109.
(95) Roy, T. K.; Gerber, R. B. Dual Basis Approach for Ab Initio Anharmonic Calculations of Vibrational Spectroscopy: Application to Microsolvated Biomolecules. *J. Chem. Theory Comput.* **2020**, *16*, 7005−7016.
(96) Pele, L.; Gerber, R. B. On the Number of Significant Mode-Mode Anharmonic Couplings in Vibrational Calculations: Correlation-Corrected Vibrational Self-Consistent Field Treatment of Di-, Tri-, and Tetrapeptides. *J. Chem. Phys.* **2008**, *128*, No. 165105.
(97) Babin, V.; Leforestier, C.; Paesani, F. Development of a "First Principles" Water Potential with Flexible Monomers: Dimer Potential Energy Surface, VRT Spectrum, and Second Virial Coefficient. *J. Chem. Theory Comput.* **2013**, *9*, 5395−5403.
(98) Babin, V.; Medders, G. R.; Paesani, F. Development of a "First Principles" Water Potential with Flexible Monomers. II: Trimer Potential Energy Surface, Third Virial Coefficient, and Small Clusters. *J. Chem. Theory Comput.* **2014**, *10*, 1599−1607.
(99) Medders, G. R.; Babin, V.; Paesani, F. Development of a "First-Principles" Water Potential with Flexible Monomers. III. Liquid Phase Properties. *J. Chem. Theory Comput.* **2014**, *10*, 2906−2910.
(100) Medders, G. R.; Paesani, F. Infrared and Raman Spectroscopy of Liquid Water through "First-Principles" Many-Body Molecular Dynamics. *J. Chem. Theory Comput.* **2015**, *11*, 1145−1154.
(101) Lambros, E.; Dasgupta, S.; Palos, E.; Swee, S.; Hu, J.; Paesani, F. General Many-Body Framework for Data-Driven Potentials with Arbitrary Quantum Mechanical Accuracy: Water as a Case Study. *J. Chem. Theory Comput.* **2021**, *17*, 5635−5650.
(102) Bull-Vulpe, E. F.; Riera, M.; Bore, S. L.; Paesani, F. Data-Driven Many-Body Potential Energy Functions for Generic Molecules: Linear Alkanes as a Proof-of-Concept Application. *J. Chem. Theory Comput.* **2022**, *19*, 4494−4509.
(103) Xie, Z.; Bowman, J. M. Permutationally Invariant Polynomial Basis for Molecular Energy Surface Fitting Via Monomial Symmetrization. *J. Chem. Theory Comput.* **2010**, *6*, 26−34.
(104) Conte, R.; Qu, C.; Houston, P. L.; Bowman, J. M. Efficient Generation of Permutationally Invariant Potential Energy Surfaces for Large Molecules. *J. Chem. Theory Comput.* **2020**, *16*, 3264−3272.
(105) Hrenar, T.; Werner, H.-J.; Rauhut, G. Towards Accurate Ab Initio Calculations on the Vibrational Modes of the Alkaline Earth Metal Hydrides. *Phys. Chem. Chem. Phys.* **2005**, *7*, 3123−3125.
(106) Pflüger, K.; Paulus, M.; Jagiella, S.; Burkert, T.; Rauhut, G. Multi-Level Vibrational SCF Calculations and FTIR Measurements on Furazan. *Theor. Chem. Acc.* **2005**, *114*, 327−332.
(107) König, C. Tailored Multilevel Approaches in Vibrational Structure Theory: A Route to Quantum Mechanical Vibrational Spectra for Complex Systems. *Int. J. Quantum Chem.* **2021**, *121*, No. e26375.
(108) Klinting, E. L.; Christiansen, O.; König, C. Toward Accurate Theoretical Vibrational Spectra: A Case Study for Maleimide. *J. Phys. Chem. A* **2020**, *124*, 2616−2627.
(109) Rauhut, G.; Hartke, B. Modeling of High-Order Many-Mode Terms in the Expansion of Multidimensional Potential Energy Surfaces: Application to Vibrational Spectra. *J. Chem. Phys.* **2009**, *131*, No. 014108.
(110) Boys, S. F. Construction of Some Molecular Orbitals to Be Approximately Invariant for Changes from One Molecule to Another. *Rev. Mod. Phys.* **1960**, *32*, 296−299.
(111) Yang, E. L.; Spencer, R. J.; Zhanserkeev, A. A.; Talbot, J. J.; Steele, R. P. Accelerating and Stabilizing the Convergence of Vibrational Self-Consistent Field Calculations Via the Direct Inversion of the Iterative Subspace (vDIIS) Algorithm. *J. Chem. Phys.* **2023**, Accepted.
(112) Weigend, F.; Häser, M. Ri-MP2: First Derivatives and Global Consistency. *Theor. Chem. Acc.* **1997**, *97*, 331−340.
(113) Distasio, R. A.; Steele, R. P.; Rhee, Y. M.; Shao, Y.; Head-Gordon, M. An Improved Algorithm for Analytical Gradient Evaluation

in Resolution-of-the-Identity Second-Order Møller-Plesset Perturbation Theory: Application to Alanine Tetrapeptide Conformational Analysis. *J. Comput. Chem.* **2007**, *28*, 839−856.

https://doi.org/10.1021/acs.jctc.3c00589
J. Chem. Theory Comput. 2023, 19, 5572−5585